Chapter 18
Terminal Set of Nonlinear Model Predictive Control with Koopman Operators

Yajing Zhang, Yangyang Feng, Shuyou Yu, and Hong Chen

Abstract A large terminal set of model predictive control results in a large region of attraction of the closed-loop systems, which can help to reduce the computational burden of the involved optimization problem. In this paper, a novel scheme is proposed to obtain a terminal set and a terminal penalty of nonlinear model predictive control. Firstly, the nonlinear system is approximated through the Koopman operator theory, whereby a linear system with unknown but bounded disturbances is generated. Then, a polytopic terminal set is obtained accordingly, where the nonlinear system is described by a linear model with disturbances. The effectiveness of the proposed scheme is demonstrated using a benchmark problem.

Keywords Terminal set · Nonlinear model predictive control · Koopman operator theory

18.1 Introduction

Model predictive control (MPC), referred to as receding-horizon control, is a widely used optimization-based control scheme. Solving an optimization problem by measuring the system state at each moment, a finite horizon control sequence is obtained accordingly. Only the first element of the obtained control sequence is applied to the system. At the next moment, the complete process is repeated with the updated system state.

Y. Zhang · Y. Feng · S. Yu · H. Chen
Department of Control Science and Engineering, Jilin University, Changchun, China

S. Yu (✉)
The Key Laboratory of Industrial Internet of Things and Networked Control, Chongqing University of Posts and Telecommunications, Chongqing, China
e-mail: shuyou@jlu.edu.cn

H. Chen
College of Electronics and Information Engineering, Tongji University, Shanghai, China

J. Berberich et al. (eds.), *Systems Theory in Data and Optimization*, Lecture Notes in Control and Information Sciences - Proceedings,
https://doi.org/10.1007/978-3-031-83191-1_18

MPC with guaranteed nominal stability [1, 2] is one of the most important model predictive control schemes, where a terminal constraint set and a terminal penalty are imposed in order to guarantee asymptotic stability. Furthermore, specific constructions of the terminal set and the terminal penalty are provided with the assumption of Lipschitz continuity. A large terminal set results in a large region of attraction for the closed-loop system, which can also reduce the online computational burden. Generally, however, finding a non-conservative terminal penalty and a terminal set is not an easy task. An approach to obtain a terminal set is developed based on a linear-quadratic regulator designed in the neighborhood of the origin, where the higher order nonlinear effect of the system is assumed to be bounded [3, 4]. Thus, it leads to a method of calculating terminal set for a large dimensional system, and terminal penalty of nonlinear systems [5], where extra degrees are added to reduce the conservativeness of the offline optimization problem.

Machine learning techniques are adopted to construct a tailored quadratic and convex terminal cost which approximates the cost-to-go function of constrained linear model predictive control frameworks [6, 7]. An algorithm is proposed, which learns the terminal penalty and adjusts the MPC parameters based on a stability metric [8]. The terminal penalty is formulated as a Lyapunov function neural network with the aim of recovering or enlarging the attraction region of the initial demonstrator using a short prediction horizon. Learning-based method is adopted to construct the terminal penalty by linking it to an infinite-horizon optimal control problem, where the Lyapunov function is the optimal cost [9].

Recently, Koopman operator theory is increasingly prevalent in engineered system design and data analysis. In this paper, motivated by linear model identification for control [10, 11], a scheme for solving the terminal set of nonlinear model predictive control is proposed. First, approximate the nonlinear system using a linear model with unknown but bounded disturbances, which act additively on the state and control inputs. Then, results are presented which permit the calculation of a maximal robust positively invariant set of discrete-time linear time-invariant system with disturbances. The maximal robust positively invariant set, also known as the 0-reachable set, is designated as the terminal set.

The remainder of the paper has the following structure. Section 18.2 defines the problem setup, and introduces the preliminaries. Section 18.3 presents the main results, including Koopman operator-based linear systems with disturbances, terminal sets of nonlinear model predictive control with a Koopman operator. To demonstrate the effectiveness of the proposed scheme, a simulation example is provided in Sect. 18.4. Section 18.5 concludes the paper.

18.2 Problem Setup and Preliminaries

Consider a discrete-time nonlinear system

$$z_{k+1} = f(z_k, v_k) \tag{18.1}$$

where $z_k \in \mathbb{R}^n$ is the state and $v_k \in \mathbb{R}^m$ is the manipulation input at the moment k. The state and control inputs are subject to the following constraints:

$$z_k \in \mathcal{Z},\ k \geq 0\,, \tag{18.2a}$$
$$v_k \in \mathcal{V},\ k \geq 0\,, \tag{18.2b}$$

where $\mathcal{Z} \subseteq \mathbb{R}^n$ and $\mathcal{V} \subseteq \mathbb{R}^m$ are the admissible sets of z_k and v_k, respectively.

Suppose that the system state z_k is measured instantaneously, and there is neither model perturbation nor external disturbance at all.

Furthermore, the following assumptions are made:

Assumption 18.1 The point $(0, 0) \in \mathbb{R}^n \times \mathbb{R}^m$ is an equilibrium point of system (18.1), i.e., $f(0, 0) = 0$, and $f : \mathbb{R}^n \times \mathbb{R}^m \longrightarrow \mathbb{R}^n$ is continuously differentiable.

Assumption 18.2 The sets of $\mathcal{Z}$ and $\mathcal{V}$ are compact, and $(0, 0) \in \mathcal{Z} \times \mathcal{V}$.

At the moment k, a finite-horizon open-loop optimization problem is defined as follows:

Problem 18.1

$$\underset{V_k}{\text{minimize}} \quad \mathcal{C}(z_k, V_k)$$

s.t.

$$z_{k+i+1|k} = f(z_{k+i|k}, v_{k+i|k}), \quad z_{k|k} = z_k, \quad i \in \mathbb{N}_{[0,N_p-1]}, \tag{18.3a}$$
$$z_{k+i|k} \in \mathcal{Z}, \qquad i \in \mathbb{N}_{[1,N_p-1]}, \tag{18.3b}$$
$$v_{k+i|k} \in \mathcal{V}, \qquad i \in \mathbb{N}_{[0,N_p-1]}, \tag{18.3c}$$
$$z_{k+N_p|k} \in \mathbb{Z}_f, \tag{18.3d}$$

where the cost functional

$$\mathcal{C}(z_k, V_k) = \sum_{i=0}^{N_p-1} \|z_{k+i|k}\|^2_{\bar{E}} + \|v_{k+i|k}\|^2_{\bar{F}} + \|z_{k+N_p|k}\|^2_{\bar{G}} \tag{18.4}$$

and $V_k := \{v_{k|k}, v_{k+1|k}, \ldots, v_{k+N_p-1|k}\}$ denotes the N_p-step control sequence, $\bar{E} \in \mathbb{R}^{n\times n}$ and $\bar{F} \in \mathbb{R}^{m\times m}$ are positive definite weighting matrices. The index $\mathbb{N}$ denotes the set of positive integers and $\mathbb{N}_{[1,N_p-1]}$ as the integers 1, 2, ..., N_p. The index $k+i|k$ denotes the values at the moment $k+i$ predicted at time k, $i \in \mathbb{N}_{[1,N_p-1]}$. The term $\mathbb{Z}_f$ is the terminal constraints set, $\|z\|^2_{\bar{G}}$ is the terminal penalty. Both $\mathbb{Z}_f$ and $\|z\|^2_{\bar{G}}$ will be determined in Sect. 18.3.

At the moment k, a optimal control sequence

$$V_k^* := \{v^*_{k|k}, v^*_{k+1|k}, \ldots, v^*_{k+N_p-1|k}\} \tag{18.5}$$

is determined by solving Problem 18.1. However, only the first control element $v^*_{k|k}$ is applied to the system. At the next moment $k+1$, the whole process is repeated with the new measurement of the system states.

Note that at the moment k, the control sequence V_k is feasible for Problem 18.1, and suppose that

(i) constraints (18.3b)–(18.3d) are satisfied;
(ii) the cost function (18.4) is finite, i.e., $\mathcal{C}(z_k, V_k) < \infty$.

At the equilibrium point (0, 0), the Jacobian linearization of system (18.1) is

$$z_{k+1} = Az_k + Bv_k, \tag{18.6}$$

where $A := \frac{\partial f}{\partial z}|_{(0,0)}$ and $B := \frac{\partial f}{\partial v}|_{(0,0)}$.

Assumption 18.3 System (18.6) is stabilizable.

Assumption 18.3 implies that a linear feedback control law $v = K_J z$ can be determined such that $A_k := A + BK_J$ is asymptoticly stable. Without loss of generality, assume further that A_k has at least one non-zero eigenvalue.

The following lemma guarantees the existence of the terminal control law $K_J z$, the terminal set $\mathbb{Z}_f$, and the terminal penalty $\|z\|^2_{\bar{G}}$ [12, 13]. Note that the terminal control law $K_J z$ is only used to determine $\mathbb{Z}_f$ and $\|z\|^2_{\bar{G}}$, and never be applied to system (18.1).

Lemma 18.1 *Suppose that Assumptions 18.1, 18.2 and Assumption 18.3 hold, and denote $\sigma_{\max}(A_k)$ as the maximum eigenvalues of matrix A_k. Then,*
(1) There exists a unique positive definite matrix $\bar{G}$ such that

$$\kappa^2 A_k^T \bar{G} A_k - \bar{G} = -(\bar{E} + K_J^T \bar{F} K_J) \tag{18.7}$$

where $\kappa \in \left(1, \frac{1}{\sigma_{\max}(A_k)}\right)$.
(2) There exists a level set $\mathbb{Z}_f \subseteq Z$, and

$$\mathbb{Z}_f := \left\{z \in \mathbb{R}^n \mid z^T \bar{G} z \leq \beta, \beta > 0\right\},$$

such that

(1) $K_J z \in \mathcal{V}$ *for any* $z \in \mathbb{Z}_f$.
(2) $\mathbb{Z}_f$ *is a positive invariant set for the original nonlinear system* (18.1), *i.e., with the feedback control law* $v = K_J z$, $z_{k+1} \in \mathbb{Z}_f$ *for any* $z_k \in \mathbb{Z}_f$.
(3) for all $z_0 \in \mathbb{Z}_f$, *and for the system* (18.1), *with the linear feedback control law* $v = K_J z$

$$\sum_{i=0}^{\infty} \|z_{i|0}\|_{\bar{E}}^2 + \|v_{i|0}\|_{\bar{F}}^2 \le z^T \bar{G} z, \tag{18.8}$$

where $z_{0|0} = z_0$ *and* $v_{i|0} = K_J z_{i|0}$.

18.3 Terminal Set of Nonlinear Systems Based on Koopman Operators

The Koopman operator is a way to handle nonlinear systems through a globally linear representation [14]. In principle, the Koopman operator transforms a finite-dimensional nonlinear system into an infinite-dimensional linear system. Alternatively, a finite approximation through a linear system with disturbances provides an effective tool on analysis and synthesis of nonlinear control systems.

For nonlinear systems (18.1), the Koopman operator ϖ is defined as follows:

$$\varpi \xi(z_k) = \xi(z_{k+1}) = \xi(f(z_k, v_k)), \tag{18.9}$$

where $\xi(\cdot)$ is an observation function.

The dynamic mode decomposition (DMD) method provides a finite-dimensional approximation to the Koopman operator ϖ [15]. The state and input data in the DMD algorithm need to be collected from the nonlinear system. Then, the state matrix identification is

$$\begin{aligned} Z_D &= [\, z_1 \; z_2 \; \cdots \; z_M \,] \\ Z_D^+ &= [\, z_2 \; z_3 \; \cdots \; z_{M+1} \,] \\ V_D &= [\, v_1 \; v_2 \; \cdots \; v_M \,], \end{aligned} \tag{18.10}$$

where $Z_D \in \mathbb{R}^{n\times M}$, $Z_D^+ \in \mathbb{R}^{n\times M}$, $V_D \in \mathbb{R}^{m\times M}$, and M is an integer.

The linear approximation of the nonlinear dynamics can be expressed as

$$Z_D^+ = A_D Z_D + B_D V_D = \begin{bmatrix} A_D & B_D \end{bmatrix} \begin{bmatrix} Z_D \\ V_D \end{bmatrix} = G\Phi, \tag{18.11}$$

where $G = \begin{bmatrix} A_D & B_D \end{bmatrix}$ and $\Phi = \begin{bmatrix} Z_D & V_D \end{bmatrix}^T$.

Note that the state matrix G can be obtained by solving the following least-square optimization problem:

$$\underset{\Phi}{minimize} \left\| Z_D^+ - G\Phi \right\|_F, \tag{18.12}$$

where $\|\cdot\|_F$ denotes the Frobenius norm.

The problem (18.12) can be solved using the pseudo-inverse matrix of Φ, i.e.:

$$G = Z_D^+ \Phi^\dagger, \tag{18.13}$$

where $\dagger$ denotes the Moore-pseudo-inverse.

The singular value decomposition of Φ is as follows:

$$\begin{aligned}\Phi &= \left[Z_D \; V_D\right]^T \\ &= U \Sigma V^T,\end{aligned}$$

where $U \in \mathbb{R}^{(n+m)\times(n+m)}$, $\Sigma \in \mathbb{R}^{(n+m)\times(n+m)}$, and $V \in \mathbb{R}^{M\times(n+m)}$.

Then, matrix G can be obtained by the following approximation:

$$\begin{aligned}G &\approx Z_D V \Sigma^{-1} U^T \\ &= Z_D V \Sigma^{-1} \left[\, U_1 \; U_2 \,\right]^T,\end{aligned}$$

where $U_1 \in \mathbb{R}^{(n+m)\times n}$, $U_2 \in \mathbb{R}^{(n+m)\times m}$.

That is,

$$\begin{aligned}A_D &\approx \tilde{A}_D = Z_D V \Sigma^{-1} {U_1}^T \\ B_D &\approx \tilde{B}_D = Z_D V \Sigma^{-1} {U_2}^T.\end{aligned}$$

Rewrite $Z_D^+ = A_D Z_D + B_D V_D$ as

$$[\, z_2 \; z_3 \; \cdots \; z_{M+1} \,] = A_D [\, z_1 \; z_2 \; \cdots \; z_M \,] + B_D [\, v_1 \; v_2 \; \cdots \; v_M \,].$$

Then, the linear model of the nonlinear system can be obtained as

$$z_{k+1} = \tilde{A}_D z_k + \tilde{B}_D v_k + w_k, \tag{18.14}$$

where w_k is the deviation between true value and its approximate value of system (18.1). Note that the presence of modeling error w_k is unavoidable due to the finite-dimensional approximation using the Koopman operator theory.

Assume that w_k is amplitude bounded, namely:

$$w_k \in \mathcal{W} = \left\{ w_k \in \mathbb{R}^n : \|w_k\|_\infty \le w^{\max} \right\},$$

where $\mathcal{W}$ is a compact set and $0 \in \mathcal{W}$.

18.3.1 Terminal Set of Nonlinear Systems

For the Koopman linear model (18.14), assume that there exists a feedback control law $v = K_D z$ such that $A_D^k := \tilde{A}_D + \tilde{B}_D K_D$ is asymptotically stable. Define $Q_D^* = \bar{E} + K_D^T \bar{F} K_D$, then the terminal gain K_D and the terminal matrix P_D satisfy [16]

$$\left(A_D^k\right)^T P_D \left(A_D^k\right) - P_D \leq -Q_D^* \tag{18.15}$$

with $P_D \in \mathbb{R}^{n\times n}$ and P_D is positive definite.

Based on the Koopman linear model with the bounded disturbance w_k, a maximal robust positive invariant set can be chosen as the terminal set. The maximal robust positive invariant set is defined as follows.

Definition 18.1 (Robust positive invariant set [17]): The set $\tilde{\mathbb{Z}}_f$ is a robust positive invariant set of the uncertain system (18.14), if $\left(\tilde{A}_D + \tilde{B}_D K_D\right) z_k + w_k \in \tilde{\mathbb{Z}}_f$ for any $z_k \in \tilde{\mathbb{Z}}_f$ and $w_k \in \mathcal{W}$.

Definition 18.2 (Maximal robust positive invariant set [17]): The robust positive invariant set $\tilde{\mathbb{Z}}_f$ is the maximal robust positive invariant set of the uncertain system (18.14), if $\tilde{\mathbb{Z}}_f$ is included in all robust positive invariant set of the uncertain system (18.14).

The maximal and polytopic positive invariant set can be described as

$$\tilde{\mathbb{Z}}_f := \left\{z \in \mathbb{R}^n | A_t z \leq b_t,\, A_t \in \mathbb{R}^{n\times n},\, b_t \in \mathbb{R}^n\right\}.$$

Note that in order to obtain the maximal robust positive invariant set, the one-step backward reachable operator is defined as follows[17]:

$$\mathrm{Pre}\,(\Omega) = \{z_k \in \mathcal{Z} | \exists K_D z_k \in \mathcal{V} : (A_D + B_D K_D)\, z_k + w_k \in \Omega, \forall w_k \in \mathcal{W}\}, \tag{18.16}$$

where Ω is a robust positive invariant set of system (18.14), Pre (Ω) is referred to as the one-step backward reachable set of the set Ω. Note that Pre (Ω) can be computed by Multi-Parametric Toolbox 3 [18].

By using (18.16), a maximal robust positive invariant set is computed by the iteration of Algorithm 18.1. Further, the terminal set of the nonlinear system (18.1) can be obtained by choosing [17]

$$\tilde{\mathbb{Z}}_f := \Omega_\infty, \tag{18.17}$$

where Ω_∞ is the maximum robust position invariant set of system (18.1), and the terminal set $\tilde{\mathbb{Z}}_f$ satisfies [17]

(i) $\tilde{\mathbb{Z}}_f \subseteq \mathcal{Z}$, $\tilde{\mathbb{Z}}_f$ is closed and the equilibrium point $(0, 0) \in \tilde{\mathbb{Z}}_f$;
(ii) $v_k = K_D z_k \subseteq \mathcal{V}$, for all $z_k \in \tilde{\mathbb{Z}}_f$;

Algorithm 18.1 Computation of the terminal set $\tilde{\mathbb{Z}}_f$

Input: $\mathcal{Z}$, $\mathcal{V}$, $\mathcal{W}$, K_D
Output: The terminal set $\tilde{\mathbb{Z}}_f$
1: Initialization. $\Omega_0 = \mathcal{Z}$.
2: Iteration procedure. At any moment $k \geq 0$, $\Omega_{k+1} = \Omega_k \cap \mathrm{Pre}\,(\Omega_k)$
3: End condition. If $\Omega_{k+1} = \Omega_k$, then set $\Omega_\infty = \Omega_{k+1}$, $\tilde{\mathbb{Z}}_f := \Omega_\infty$. Else, set $k = k+1$, and go to Step 2.

(iii) $A_D^k z_k \in \tilde{\mathbb{Z}}_f$.

Remark 18.1 Both the invariance of terminal sets and the cost from the end of the prediction horizon to infinity are guaranteed by the terminal control law $K_D z$, where the linear control gain K_D is calculated by (18.15) offline.

18.4 Numerical Example

In this section, a nonlinear system is used to verify the effectiveness of the proposed scheme, in which dynamics is

$$\begin{cases} \dot{z}_{k+1}^1 = z_k^1 + 0.1 z_k^2 + 0.1 v_k(\mu + (1-\mu) z_k^1) \\ \dot{z}_{k+1}^2 = z_k^2 + 0.1 z_k^1 + 0.1 v_k(\mu - 4(1-\mu) z_k^2) \end{cases} \tag{18.18}$$

where $\mu \in (0, 1)$. Terms of $z = \begin{bmatrix} z^1 & z^2 \end{bmatrix}^T$ and v represent the state and input, respectively. Note that the nonlinear system (18.18) is unstable and its linearized system is stabilizable. Moreover, the input and state of the system (18.18) are constrained as

$$-2 \leq v \leq 2$$
$$\begin{bmatrix} -1 \\ -1 \end{bmatrix} \leq \begin{bmatrix} z_k^1 \\ z_k^2 \end{bmatrix} \leq \begin{bmatrix} 1 \\ 1 \end{bmatrix}.$$

Scenario 18.1 The parameter $\mu = 0.5$.

The collected datasets consist of 20 episodes, each containing data of 400 time steps. The initial state is randomly chosen within the range of $[-1,\ 1]$, and the control input is within the range of $[-2,\ 2]$.

The matrices $\tilde{A}_D$, $\tilde{B}_D$, and the bounded disturbance w_k by the Koopman operator theory are calculated as

$$\tilde{A}_D = \begin{bmatrix} 1.0150 & 0.0965 \\ 0.0693 & 1.0379 \end{bmatrix},\ \tilde{B}_D = \begin{bmatrix} 0.0500 \\ 0.1035 \end{bmatrix},\ \|w_k\|_\infty \leq 0.1.$$

The weighting matrices $\bar{E}$ and $\bar{F}$ in the optimization problem of MPC are given as

$$\bar{E} = \begin{bmatrix} 0.5 & 0 \\ 0 & 0.5 \end{bmatrix}, \quad \bar{F} = 1.$$

Further, the terminal gain K_D and the terminal matrix P_D are calculated offline by (18.15), and

$$K_D = \begin{bmatrix} 1.3006 & 1.6392 \end{bmatrix}, \; P_D = \begin{bmatrix} 12.1326 & 8.6059 \\ 8.6059 & 13.8252 \end{bmatrix}.$$

As a comparison, the matrices A and B by the Jacobian linearization method at the equilibrium point (0, 0) are calculated as

$$A = \begin{bmatrix} 1.005 & 0.1002 \\ 0.1002 & 1.0005 \end{bmatrix}, \; B = \begin{bmatrix} 0.0526 \\ 0.0526 \end{bmatrix}.$$

Similarly, the terminal gain K_J and the terminal matrix $\bar{G}$ are calculated using Lemma 18.1, that is,

$$K_J = \begin{bmatrix} 2.118 & 2.118 \end{bmatrix}, \; \bar{G} = \begin{bmatrix} 16.5926 & 11.359 \\ 11.359 & 16.5926 \end{bmatrix}, \quad \beta = 0.7.$$

Under the same input, a simulation experiment is implemented to compare the evolution of the nonlinear system (18.18), the Koopman linear system, and the Jacobian linearization system. The simulation results are shown in Fig. 18.1. It can be seen that the Koopman linear model and the Jacobian linearization model can accurately approximate the nonlinear system (18.18).

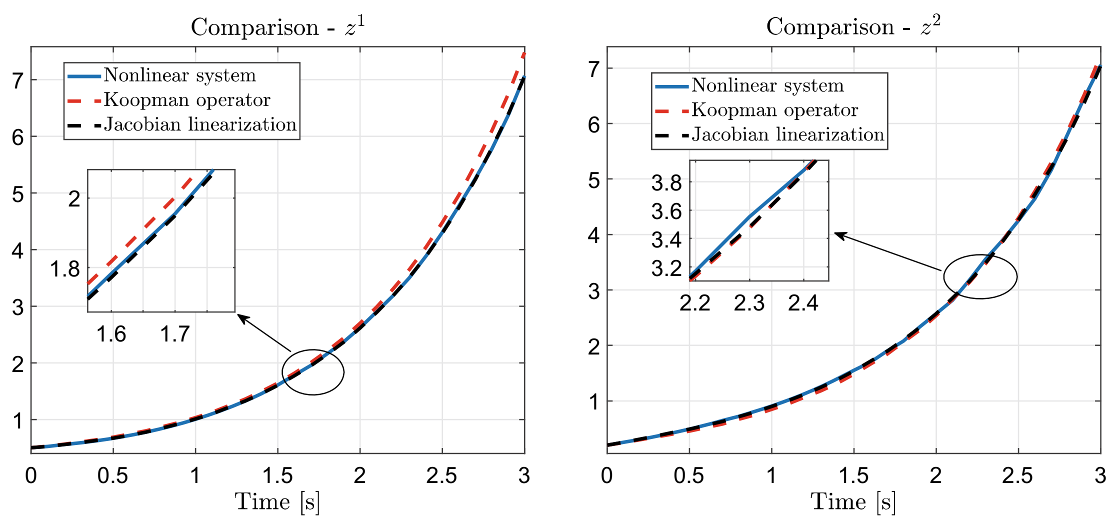

Fig. 18.1 Scenario 18.1 Validation of the Koopman linear model and the Jacobian linearization model ($\mu = 0.5$)

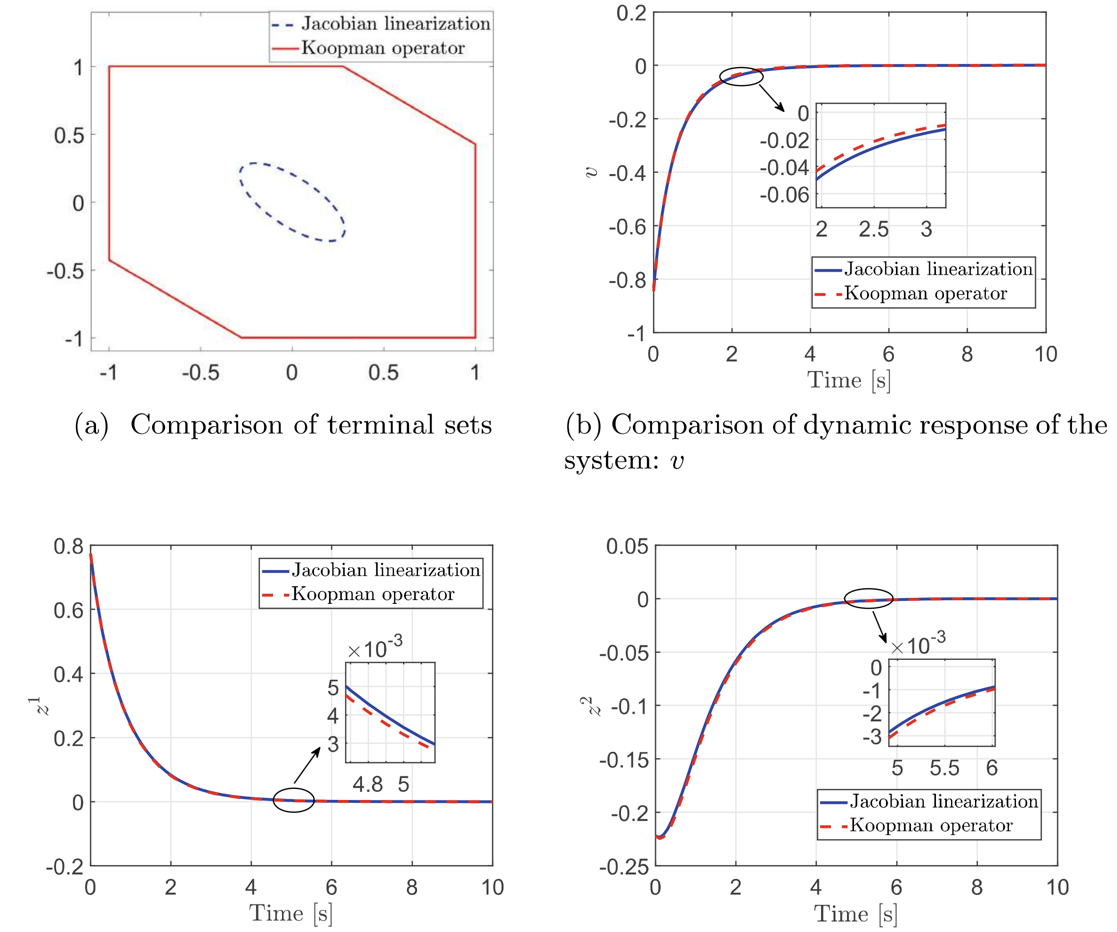

(a) Comparison of terminal sets

(b) Comparison of dynamic response of the system: v

(c) Comparison of dynamic response of the system: z^1

(d) Comparison of dynamic response of the system: z^2

Fig. 18.2 Simulation results of Scenario 18.1 for the initial state $z_0 = [0.774 \quad -0.222]^T$ and the prediction horizon $N_p = 15$

The terminal set $\tilde{\mathbb{Z}}_f$ computed based on the Koopman linear model with the bounded disturbance w_k and the terminal set $\mathbb{Z}_f$ computed based on the Jacobian linearization model are shown in Fig. 18.2a. It can be found that the terminal set $\tilde{\mathbb{Z}}_f$ computed based on the Koopman linear model is larger. Figure 18.2b–d shows the evolution of control input, and the dynamic response of the system at the initial state $z_0 = [0.774 \quad -0.222]^T$, while the prediction horizon $N_p = 15$. The dynamic response of the system with the terminal ingredients obtained based on the Koopman linear model is marked as the red solid line, and the dynamic response of the system with the terminal ingredients obtained based on the Jacobian linearization model is marked as the blue dashed line. It can be observed that the dynamic response trajectory of the system can asymptotically converge to the equilibrium point within the control input limitations.

Figure 18.3 shows the dynamic response of the system at the initial state $z_0 = [1 \quad -1]^T$, while the prediction horizon $N_p = 10$. Figure 18.3a shows that the control

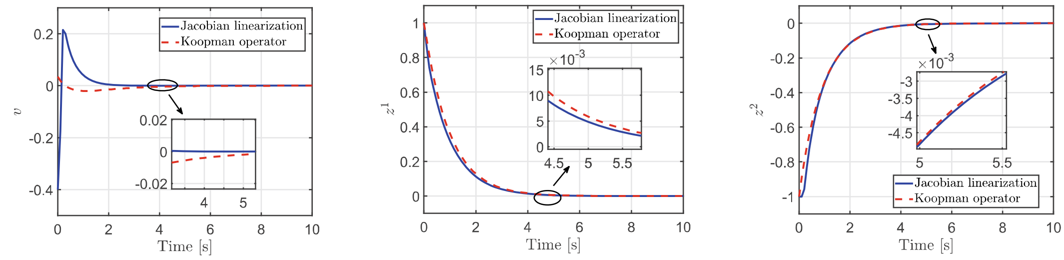

(a) Comparison of dynamic response of the system: v (b) Comparison of dynamic response of the system: z^1 (c) Comparison of dynamic response of the system: z^2

Fig. 18.3 Simulation results of Scenario 18.1 for the initial state $z_0 = [1 \quad -1]^T$ and the prediction horizon $N_p = 10$

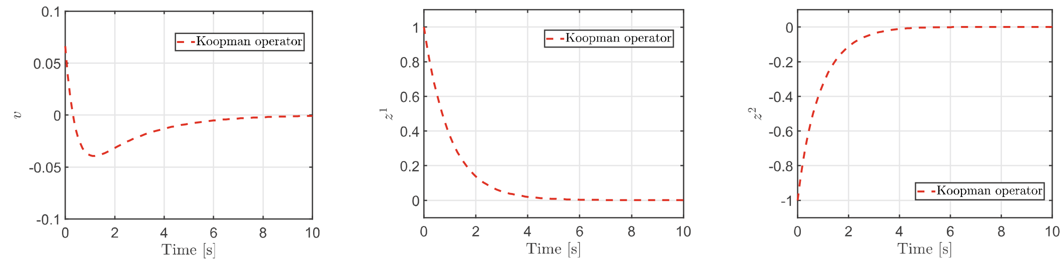

(a) Comparison of dynamic response of the system: v (b) Comparison of dynamic response of the system: z^1 (c) Comparison of dynamic response of the system: z^2

Fig. 18.4 Simulation results of Scenario 18.1 for the initial state $z_0 = [1 \quad -1]^T$ and the prediction horizon $N_p = 5$

inputs at the initial moment solved by the Problem 18.1 with the terminal ingredients obtained based on the Koopman linear model is smoother than using the terminal ingredients obtained based on the Jacobian linearization model. However, while the prediction horizon $N_p = 5$, Problem 18.1 with the terminal ingredients obtained based on the Jacobian linearization model has no feasible solution at the initial moment. Problem 18.1 with the terminal ingredients obtained based on the Koopman linear model has feasible solution at the initial time instant. Figure 18.4 shows the simulation results of the proposed control scheme for the initial state $z_0 = [1 \quad -1]^T$ while $N_p = 5$.

Scenario 18.2 The parameter $\mu = 0.8$.

The collected datasets consist of 25 episodes, each containing data of 610 time steps. The initial state is randomly chosen within the range of $[-1,\ 1]$, and the control input is allowed within the range of $[-2,\ 2]$.

The matrices $\tilde{A}_D$, $\tilde{B}_D$ and the bounded disturbance w_k by the Koopman operator theory are calculated as

$$\tilde{A}_D = \begin{bmatrix} 1.0061 & 0.0993 \\ 0.0968 & 1.0130 \end{bmatrix},\ \tilde{B}_D = \begin{bmatrix} 0.0840 \\ 0.0875 \end{bmatrix},\ \|w_k\|_\infty \le 0.1.$$

The weighting matrices $\bar{E}$, $\bar{F}$ and the prediction horizon N_p in the optimization problem of MPC are given as

$$\bar{E} = \begin{bmatrix} 1 & 0 \\ 0 & 1 \end{bmatrix}, \quad \bar{F} = 1, \quad N_p = 15.$$

Further, the terminal gain K_D and the terminal matrix P_D are calculated by (18.15) offline, that is,

$$K_D = \begin{bmatrix} 1.3116 & 1.3718 \end{bmatrix}, \; P_D = \begin{bmatrix} 10.0617 & 7.4326 \\ 7.4326 & 10.7298 \end{bmatrix}.$$

As a comparison, the matrices A and B by the Jacobian linearization method at the equilibrium point (0, 0) are calculated as

$$A = \begin{bmatrix} 1.005 & 0.1002 \\ 0.1002 & 1.0005 \end{bmatrix}, \; B = \begin{bmatrix} 0.0841 \\ 0.0841 \end{bmatrix}.$$

Similarly, the terminal gain K_J and the terminal matrix $\bar{G}$ are calculated using Lemma 18.1 as

$$K_J = \begin{bmatrix} 1.2901 & 1.3062 \end{bmatrix}, \; \bar{G} = \begin{bmatrix} 9.6999 & 6.9486 \\ 6.9486 & 9.8201 \end{bmatrix}, \quad \beta = 5.2035.$$

While $\mu = 0.8$, the simulation experimental result is shown in Figs. 18.5 and 18.6. Figure 18.5 shows that the Koopman linear model and the Jacobian linearization model can accurately approximate the nonlinear system (18.18) under Scenario 18.2. Figure 18.4a shows that the proposed method can obtain a larger terminal set under

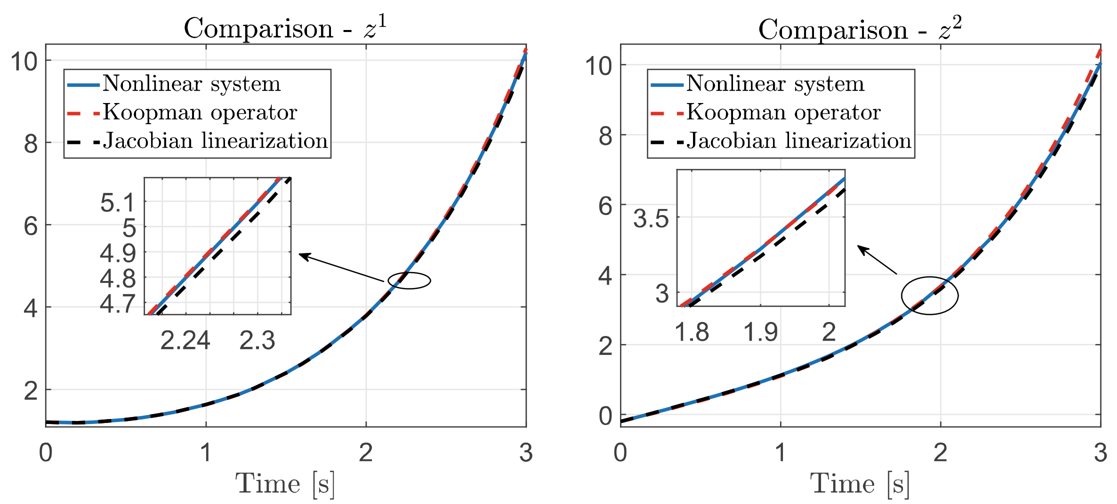

Fig. 18.5 Scenario 18.2 Validation of the Koopman linear model and the Jacobian linearization model ($\mu = 0.8$)

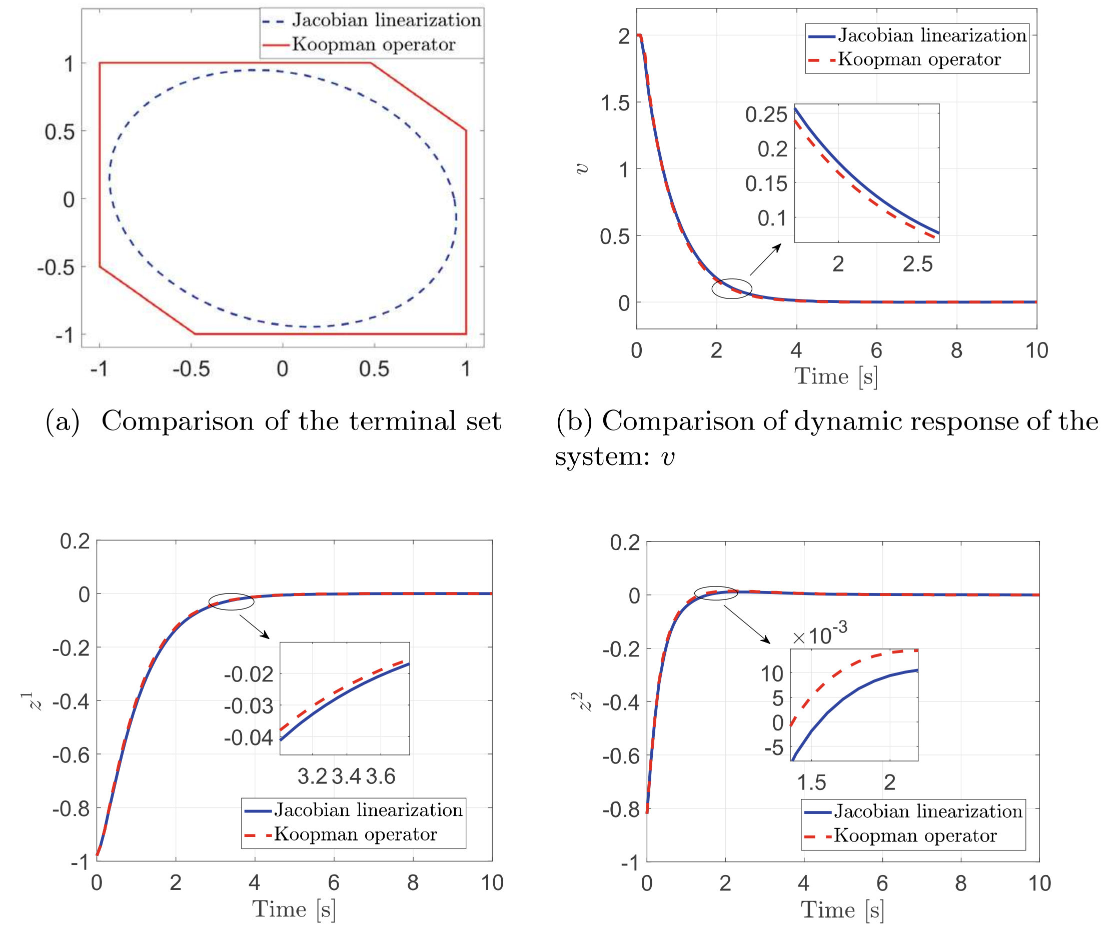

(a) Comparison of the terminal set

(b) Comparison of dynamic response of the system: v

(c) Comparison of dynamic response of the system: z^1

(d) Comparison of dynamic response of the system: z^2

Fig. 18.6 Simulation results of Scenario 18.2 for the initial state $z_0 = [-0.98 \quad -0.82]^T$ and the prediction horizon $N_p = 15$

Scenario 18.2. Figure 18.4b–d shows that the dynamic response trajectory of the system can asymptotically converge to the equilibrium point under the control input limitations, where the initial state of the system is set as $z_0 = [-0.98 \quad -0.82]^T$.

18.5 Conclusion

In this paper, a scheme to solve the terminal set of model predictive control of nonlinear systems with constraints was proposed. The considered nonlinear system was approximated by a Koopman operator dynamics model, which was a linear system with bounded disturbances. Then, an algorithm to offline determine the terminal cost, terminal set, and terminal control law was developed, where the terminal set was a maximal robust invariant set of the linear dynamical model with the terminal control law, and the terminal penalty was the related cost function. A simulation example under different scenarios demonstrated the effectiveness of the proposed scheme.

Funding This work was supported by the National Natural Science Foundation of China (No. U62473167) and the Science Foundation of Jilin Province (No.20240402079GH), China.

References

1. Chen, H., Allgöwer, F.: A quasi-infinite horizon nonlinear model predictive control scheme with guaranteed stability. Automatica **34**(10), 1205–1217 (1998)
2. Mayne, D.Q., Rawlings, J.B., Rao, C.V., Scokaert, P.O.M.: Constrained model predictive control: stability and optimality. Automatica **36**(6), 789–814 (2000)
3. Rajhans, C., Griffith, D., Patwardhan, S.C., Biegler, L.T., Pillai, H.K.: Two approaches for terminal region characterization in discrete time quasi-infinite horizon NMPC. In: 6th IFAC Conference on Nonlinear Model Predictive Control, IFAC, Madison, WL, USA (2018)
4. Rajhans, C., Griffith, D.W., Patwardhan, S.C., Biegler, T., Pillai, H.K.: Terminal region characterization and stability anslysis of discrete time quasi-infinite horizon nonlinear model predictive control. J. Proc. Contr. **483**, 30–52 (2019)
5. Yu, S., Feng, Y., Kim, J.S., Chen, H.: Computation of terminal set for nonlinear model predictive control. ACTA Automatica Sinica **48**(1), 144–151 (2022)
6. Abdufattokhov, S., Zonon, M., Bemproad, A.: Learning convex terminal costs for complexity reduction in MPC. In: Proc, pp. 2163–2168. Amer. Contr. Conf, Austin, Texas (2021)
7. Abdufattokhov, S., Zonon, M., Bemproad, A.: Learning Lyapunov terminal costs from data for complexity reduction in nonlinear model predictive control. Int. J. Robust Nonlinear Control (2024). https://doi.org/10.1002/rnc.7411
8. Mittal, M., Gallieri, M., Quaglino, A., Salehian, S.S.M., Koutnik, J.: Neural Lyapunov model predictive contro: Learning safe global controllers from sub-optimal examples. In: arXiv:2002.10451v2 (2021)
9. Moreno-Mora, F., Beckenbach, L., Streif, S.: Predictive control with learning-based terminal costs using approximate value iteration. IFAC PaperOnLine **56–2**, 3874–3879 (2023)
10. Milan, K., Igor, M.: Linear predictors for nonlinear dynamical systems: Koopman operator meets model predictive control. Automatica **93**, 149–160 (2018)
11. Zhang, X., Pan, W., Scattolini, R., Yu, S., Xu, X.: Robust tube-based model predictive control with koopman operators. Automatica **137**(110), 114 (2022)
12. Yu, S., Hou, C., Qu, T., Chen, H.: A revisit to mpc of discrete-time nonlinear systems. In: 2015 IEEE International Conference on Cyber Technology in Automation, Control, and Intelligent Systems (CYBER), pp 7–12 (2015). https://doi.org/10.1109/CYBER.2015.7287901
13. Yu, S., Qu, T., Xu, F., Chen, H., Hu, Y.: Stability of finite horizon model predictive control with incremental input constraints. Automatica **79**, 265–272 (2017)
14. Korda, M., Mezić, I.: Linear predictors for nonlinear dynamical systems: Koopman operator meets model predictive control. Automatica **93**, 149–160 (2018)
15. Proctor, J.L., Brunton, S.L., Kutz, J.N.: Dynamic mode decomposition with control (2014). https://arxiv.org/abs/1409.6358
16. Feng, Y., Shuyou, Yu.Y., Li, Shi S., Yu, J., Chen, H.: Distributed mpc of vehicle platoons considering longitudinal and lateral coupling. IEEE Trans. Intell. Transp. Syst. **25**(3), 2293–2310 (2024)

17. Borrelli, F., Bemporad, A., Morari, M.: Predictive control for linear and hybrid Systems. Cambridge University Press, Cambridge, U.K. (2017)
18. Herceg, M., Kvasnica, M., Jones, C., Morari, M.: Multi-parametric toolbox 3.0. In: Proc. Eur. Control Conf., Zurich, Switzerland (2013). https://www.mpt3.org/